Accepted Manuscript

Molecular insight into the amine-water interaction: A combined vibrational, energetic and NBO / NEDA study

A.J. Lopes Jesus, J.S. Redinha
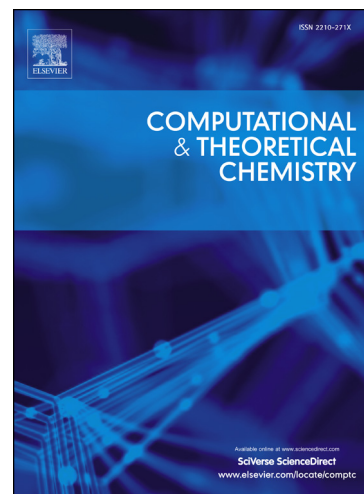
Please cite this article as: A.J. Lopes Jesus, J.S. Redinha, Molecular insight into the amine-water interaction: A combined vibrational, energetic and NBO / NEDA study, *Computational & Theoretical Chemistry* (2013), doi: http://dx.doi.org/10.1016/j.comptc.2013.09.006

Molecular insight into the amine-water interaction:
A combined vibrational, energetic and NBO / NEDA study

A. J. Lopes Jesus*[a,b] and J. S. Redinha[b]

[a] *Faculty of Pharmacy, University of Coimbra, 3004-295, Coimbra, Portugal.*

[b] *Department of Chemistry, University of Coimbra, 3004-535, Coimbra, Portugal.*

Corresponding author:
E-mail address: ajorge@qui.uc.pt

Abstract

Hydrates of the neutral and protonated cyclohexylamine and of the cyclohexyldiamine isomers in the neutral, mono and diprotonated forms are studied theoretically at the B3LYP/aug-cc-pVDZ level of theory. Vibrational Analysis of the optimized complexes shows variations in the frequency and intensity of the N–H and O–H stretching modes induced by charge variation and groups' proximity. These results are quantified by calculating the energies of complex formation ($\Delta E_{complex}$). It is shown that the values obtained for this quantity result from the balance between water association (ΔE_{ass}) and amine-water interactions (ΔE_{int}). Amino groups' approximation leads to values of ΔE_{int} different from those calculated by adding their individual contribution. This behavior is explained by the application of the Natural energy decomposition analysis (NEDA) and Natural Bond Orbitals (NBO) theory to the complexes and to the amine-water pairs. The Atoms in Molecules (AIM) theory is also used to interpret the hydration of the diprotonated diamines. Special attention is given to the characterization of the hydrogen bonds' nature, as well as to the effect of the hydrogen bonding cooperativity and charges proximity on the amine-water interaction.

1. Introduction

Many molecules of biological interest contain two or more primary amino groups in their chemical structure, which can be in either neutral ($-NH_2$) or charged ($-NH_3^+$) forms and occupying different relative positions [1-3]. The simplest examples are the diamines which find numerous applications in different fields [4-9]. Because of the relevance of these compounds in aqueous media, the understanding of their hydration structure is a matter of utmost importance.

Some experimental and theoretical studies of the hydration of diamines reveal that their interaction with water may be influenced by various molecular features, namely the spatial orientation and configuration of the groups, as well as their relative distance [10-15]. Recently, the authors have studied the structure of protonated cyclohexyldiamines in highly dilute aqueous solutions using molecular dynamics simulations [16]. From the radial distribution functions and water residence times it has been shown that the groups interfer with each other.

The aim of this paper is to establish a molecular picture of the variations of the interaction of the diamines with the surrounding water molecules induced by the mutual influence between charged or uncharged amino groups. In order to achieve this, a theoretical investigation of hydrates of cyclohexyldiamine isomers in neutral, mono and diprotonated forms will be performed using the density functional theory (DFT) method. These systems simulate the most common situations concerning the amino groups' interference in aqueous solution, thus providing valuable information about the structure of polyamines in this medium. Furthermore, they are computationally advantageous because the rigidity of the cyclohexyl ring considerably restricts their conformational freedom. To be used as reference, hydrates of the neutral and charged cyclohexylamine will be included in this study. For the sake of simplicity, from here on,

we will use the term amine (abbreviated as "Am") to refer to the molecules under study in general terms.

The structure of the complexes is essentially determined by the Am-water and water-water hydrogen bonds, seldom by Am-Am intramolecular H-bonds. Methods specially recommended to study this type of interaction will be employed in the present research, namely infrared spectroscopy, Natural Energy Decomposition Analysis (NEDA) [17-19] and Natural Bond Orbital theory (NBO) [20-22]. The first is commonly used as a fingerprint of the H-bonds and the two latter are excellent approaches to characterize the nature of these bonds.

2. Computational methods

The molecules used in this research are the cyclohexylamine (CHA) and the following cyclohexyldiamine (CHDA) isomers in both basic and acid forms: *trans*-1,4-(t14), *cis*-1,3- (c13) and *trans*-1,2-cyclohexyldiamine (t12). The mono and diprotonated forms are denoted by adding "+" or "2+" as superscript, respectively. The Am-water complexes were constructed by placing three water molecules around each amino group. Details of this procedure are given in a previous authors' paper [16]. Monoamine complexes are designated as $CHA(H_2O)_3$ or $CHA^+(H_2O)_3$ and the diamine ones as $CHDA(H_2O)_6$, $CHDA^+(H_2O)_6$ and $CHDA^{2+}(H_2O)_6$. For specific diamine complexes we use the abbreviated name of the diamine (t12, c13 or t14).

The complexes were fully optimized at the DFT level using the B3LYP hybrid functional [23-25] and the aug-cc-pVDZ basis set of Dunning and co-workers [26, 27]. Basis set superposition error (BSSE) has been removed by employing the Boys and Bernardi counterpoise correction method [28]. This correction has been included in each step of the gradient optimization and each water molecule has been taken as an individual fragment. Vibrational analysis was carried out at the same level of theory in

order to verify the nature of optimized complexes and to calculate the harmonic frequencies and intensities of the N–H and O–H stretching vibration modes. The calculated stretching frequencies have been multiplied by a scale factor of 0.9698 [29] to account for the anharmonicity effect, plus the use of an incomplete basis set and approximate method to solve the Schrödinger equation [29-31]. These calculations were performed using the Gaussian 03 program package [32]. Vibrations were approximately described by visual examination of the animated normal modes using the GaussView v.4.1 molecular visualization program [33].

Natural Bond Orbital analysis (NBO) and Natural energy decomposition analysis (NEDA) were run on the optimized complexes, as well as on all Am-water pairs retaining the complex geometry. These calculations were carried out at the B3LYP/aug-cc-pVDZ level using the NBO 5.G program [34] implemented in the GAMESS software package [35]. The $CHA^+(H_2O)_3$ and $CHDA^{2+}(H_2O)_6$ complexes were also analyzed using the Atoms in Molecules (AIM) theory. Characterization of the bond critical points (BCP) of the N^+–H bonds was carried out with the program EXTREME [36, 37].

In order to check the reliability of the B3LYP/aug-cc-pVDZ model chemistry in the prediction of the energetics of the Am-water interactions, we have calculated the values of the enthalpy and Gibbs energy of complexation for various alkylamines and alkyldiamines and have compared these values with those experimentally available for these systems [12, 13, 38, 39]. A total of eleven complexes containing different number of water molecules have been considered, including monocharged monoamines ($CH_3NH_3^+$, n-$C_3H_7NH_3^+$ and n-$C_6H_{13}NH_3^+$), a monocharged diamine [$NH_2(CH_2)_2NH_3^+$] and a di-charged diamine [$NH_3^+(CH_2)_6NH_3^+$]. The result of this comparison is given as supplementary material (Table S.1). A mean deviation of ~ 5 kJ mol^{-1} was found to

exist between the experimental and theoretical values, meaning that the energies of the Am-water interactions are satisfactorily quantified at the B3LYP/aug-cc-pVDZ level of theory.

3. Results and discussion

3.1. Vibrational analysis and structure of the amine-water complexes

The optimized geometries of the complexes under study are displayed in Figure 1 together with the atom numbering scheme. Water molecules are designated as w_i where i is the corresponding oxygen atom labeling. In Tables 1-3 are given the wavenumbers, intensities and approximate description of the N–H and O–H stretching vibrations. The simulated infrared spectra of the different complexes are given as supplementary information (Figures S.1 to S.3).

For all complexes the higher frequency vibrations (3775-3550 cm^{-1}) are assigned to the stretching of "free" OH groups (not acting as H-bond donors) or to the antisymmetric and symmetric stretching of "free" water molecules. Modes ranging from 3550 to 2900 cm^{-1} correspond to the stretching vibrations of the H-bonded hydroxyl and amino groups. To the best of our knowledge, no experimental spectral data are available for the systems under study. The only available experimental data that could be compared with our results are the vibrational predissociation spectroscopic studies performed for some protonated alkyldiamines [40]. Generally, a good agreement is found between the calculated and experimental N-H and O-H stretching vibrations, which indicates that the theoretical frequencies are correctly scaled.

It is well established that an H-bond formation is generally accompanied by the displacement of the stretching vibration of the H-donor group towards lower frequencies and by an increase of its intensity [41-43]. Taking as reference the stretching vibration of a "free" group (v^o), the frequency shift (Δv) is given by $\Delta v = v^o - v$.

For the groups under consideration, the values of ν^o are: $\nu^o(OH) \approx 3748$ cm^{-1}, $\nu^o_{as}(NH_2)$ ≈ 3440 cm^{-1}, $\nu^o_s(NH_2) \approx 3359$ cm^{-1}, $\nu^o_{as}(NH_3^+) \approx 3372$ cm^{-1}, $\nu^o_s(NH_3^+) \approx 3279$ cm^{-1}. The first corresponds to the mean value of the free OH-stretching vibrations calculated for all complexes while the others were obtained from the spectra of the isolated monoamines (see supplementary information, Table S.2).

Although to higher $\Delta\nu$ corresponds in general to stronger H-bonds, it is rather difficult to establish a quantitative relationship between this quantity and the H-bond energy. On the one hand, the stretching of the donor group may be involved in more than one vibration mode (see Tables 1-3); on the other, the proportionality constant relating both quantities may vary from one system to the other. Nevertheless, the ordering of the $\Delta\nu$ values is certainly very useful when studying the H-bonds' network in the hydrates we are investigating.

Let us first consider the spectral features of the CHA(H$_2$O)$_3$ complex such that we can visualize the local hydration structure of a neutral amino group free from the interference of other similar groups. The sequence of the $\Delta\nu$ values is the following: O$_1$H⋯N (751 cm^{-1}) $\gg$ O$_2$H⋯O$_1$ (451-465 cm^{-1}) > O$_3$H⋯O$_2$ (365 cm^{-1}) $\gg$ N$_{1a}$H⋯O$_3$ (31–77 cm^{-1}). Therefore, the H-bond between w$_1$ and the amino group is the strongest one, followed by those connecting the three water molecules. These, are in turn much stronger than that between N$_{1a}$H and w$_3$. In this complex, the arrangement of the water molecules around the amino group is strongly stabilized by hydrogen bonding cooperativity [44-50]. This effect is well evidenced by the displacement to lower wavenumbers of $\nu(O_2H)$ and $\nu(O_3H)$ relative to the bonded OH group in the water dimer (3569 cm^{-1}) and of $\nu(O_1H)$ relative to the CHA monohydrate (3347 cm^{-1}). The OH-stretching frequencies for these references were calculated by the authors at the level of theory referred to above.

7

The vibrational features of the $t14(H_2O)_6$ complex are identical to those described for $CHA(H_2O)_3$, revealing that the NH_2 groups are too far apart to influence each other. On the contrary, mutual influence is found to exist when the groups occupy the 1,3-positions. Indeed, comparing the main vibrations of $c13(H_2O)_6$ with those of $14(H_2O)_6$ one can see that in the first complex they fall into a much narrower region. This is caused by the large blue-shift of the stretching vibrations involving the OH groups connected to the nitrogen atoms (>230 cm^{-1}). Hence, we can conclude that the groups' proximity reduces the nitrogen lone-pair capacity to be an acceptor of water. Structurally, the hydration layer of $c13(H_2O)_6$ is characterized by a cyclic tetramer of water molecules cooperatively H-bonded. Two of them (w_1 and w_3) are H-bond donors to NH_2 and simultaneously are H-acceptors from the two outermost water molecules (w_5 and w_6). No $N–H\cdots O_w$ H-bonds are found to exist in this complex.

The close proximity of the NH_2 groups in $t12(H_2O)_6$ modifies slightly its vibrational and structural features relative to the previous complex. The vibrations spread either to lower or higher frequencies as a consequence of the wider range of H-bonds strengths. In addition, the lower frequency vibration is $\nu(O_5H)$ due to the strong H-bond between w_3 (double proton donor) and w_5 (double proton acceptor).

Considering now the $CHA^+(H_2O)_3$ complex (C_s symmetry, see Figure 1), the presence of the charge increases the proton donor ability of the amino group. Indeed, the values of $\Delta\nu$ for the $\nu_{as}(NH_3^+)$ and $\nu_s(NH_3^+)$ vibrations, 206 and 162 cm^{-1}, respectively, are much higher than those found for the neutral monoamine complex. The interaction of the protonated amino group with the water molecules takes place through three strong $N^+–H\cdots O_w$ interactions, commonly called charge-assisted H-bonds [39, 51-54].

In the monoprotonated complexes we have a charged and a neutral amino group located at different distances. From the comparison of their infrared spectra with those

of the charged and neutral monoamine complexes, important data can be extracted concerning the mutual influence of the groups on the Am-water hydrogen bonds. When the groups occupy the most remote positions [t14$^+$(H$_2$O)$_6$], ν(N$^+$H$_{1a}$) is red-shifted by more than 109 cm^{-1} relative to CHA$^+$(H$_2$O)$_3$. This is an indication that the donor ability of N$^+$–H$_{1a}$ is strengthened in the presence of the NH$_2$ group. Since the groups are too far apart to interact directly with one another, such influence can only be made through the cooperative effect along the water bridge connecting both groups (see Figure 1). On the contrary, the presence of NH$_3$$^+$ weakens the NH$_2$–water interactions as can be seen by comparing ν(O$_5$H) in this complex with ν(O$_1$H) in CHA(H$_2$O)$_3$.

When the NH$_3$$^+$ and NH$_2$ groups are in the 1,3-positions, two water bridges are formed between them. The variations of the N$^+$–H stretching vibrations relative to CHA$^+$(H$_2$O)$_3$ indicates a synergetic effect of NH$_2$ on NH$_3$$^+$ along the 3-water molecules bridge and an anti-synergetic one along the 2-water molecules bridge. The interference of NH$_3$$^+$ on NH$_2$ is manifested by the displacement of ν(O$_5$H) towards lower frequencies relative to ν(O$_1$H) in CHA(H$_2$O)$_3$. This shift is explained by the double proton acceptor character of w$_5$.

Regarding the protonated vicinal isomer, the proximity of the amino groups gives rise to the establishment of an N$^+$–H$_{1b}$···N intramolecular H-bond which is characterized by the vibration at 3177 cm^{-1}, ν(N$^+$H$_{1b}$). In the spectrum of the isolated molecule this mode is found at 2940 cm^{-1} (see supplementary information, Figure S.2) which means that the intramolecular H-bond is not broken by the complex formation but its strength decreases by 237 cm^{-1}. The persistence of this H-bond in the complex prevents the participation of the NH$_2$ group in the water bridging.
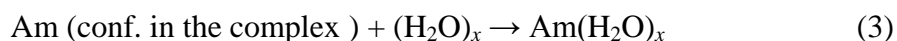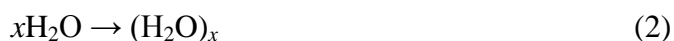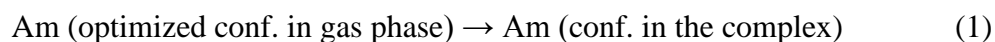
As far as the diprotonated complexes are concerned, the 3500-3000 cm^{-1} spectral region is dominated by the NH$_3$$^+$ stretching vibrations. Since the t14^{2+}(H$_2$O)$_6$ and

c13^{2+}(H$_2$O)$_6$ complexes have respectively C_{2h} and C_s symmetry, the ν_{as}(NH$_3^+$) and ν_s(NH$_3^+$) modes of one group are coupled with the equivalent modes of the other group in in-phase or out-of-phase vibrations (see Table 3). These vibrations are displaced towards lower frequencies relative to CHA$^+$(H$_2$O)$_3$. Also, the intensities are much higher than those in the spectrum of the monoamine. It is noteworthy that these spectral modifications increase as the groups approximate to each other. That is, the H-bonds between a NH$_3^+$ group and the water molecules are strengthened in the presence of a second NH$_3^+$ group. This effect was previously noted by Kebarle *et al.* on studying the thermochemistry of diprotonated alkyldiamines using the electrospray generated ions technique [12]. It was attributed to the Coulombic repulsion between the charged groups. This effect will be interpreted later in this chapter by applying the NBO and AIM theories.

3.2. *Energetics of complex formation*

Infrared spectroscopy allowed a description of the H-bonds network in the Am-water complexes and an estimation of their strength expressed in terms of frequency displacement. Thermodynamics can supply energetic information about these H-bonds.

The complexation of a mono or diamine in the neutral or protonated forms with x isolated water molecules can be divided into the following steps:

$$\text{Am (optimized conf. in gas phase)} \rightarrow \text{Am (conf. in the complex)} \qquad (1)$$

$$x\text{H}_2\text{O} \rightarrow (\text{H}_2\text{O})_x \qquad (2)$$

$$\text{Am (conf. in the complex)} + (\text{H}_2\text{O})_x \rightarrow \text{Am(H}_2\text{O})_x \qquad (3)$$

(H$_2$O)$_x$ represents the envelope of x-water molecules surrounding the amine and Am(H$_2$O)$_x$ the complex. Energetically, (1) corresponds to the energy of conformational change of the amine upon complexation, ΔE_{conf} ; (2) to the association energy of the x-water molecules to give the water envelope, ΔE_{ass}; and (3) to the energy of the Am-

water interactions, ΔE_{int}. The energy of complex formation ($\Delta E_{complex}$) can therefore be expressed as:

$$\Delta E_{complex} = \Delta E_{conf} + \Delta E_{ass} + \Delta E_{int} \qquad (4)$$

The values calculated for all quantities included in this equation are graphically represented in Figure 2. As can be seen from this figure, ΔE_{conf} has a negligible contribution on $\Delta E_{complex}$. This quantity is therefore fundamentally determined by ΔE_{ass} and ΔE_{int}. In what follows, the role of these terms in the energy of complex formation will be discussed.

In CHA(H$_2$O)$_3$, the contribution of ΔE_{ass} and ΔE_{int} is similar. When a second NH$_2$ group is added at the most remote position, both energetic terms are approximately twice as much as those calculated for CHA(H$_2$O)$_3$ and their relative weight is preserved. This is an indication that the two NH$_2$ groups do not disturb each other, which is supported by the spectroscopic data. The mutual influence between the NH$_2$ groups when they occupy the 1,3- and 1,2-positions is manifested by an increase of the water association and a decrease of the Am-water interaction. A certain compensation of both effects leads to small variations of $\Delta E_{complex}$ among the different CHDA(H$_2$O)$_6$ complexes.

Previously, we have determined experimentally the enthalpies of hydration for the *trans*-1,4- and *cis*-1,2-CHDA isomers and from this dada the enthalpies of solute-solvent interaction (ΔH_{int}) were calculated [55]. Values of $\Delta H_{int} = -125.9$ kJ mol^{-1} and -108.0 kJ mol^{-1} respectively were obtained for the remote and vicinal isomer. Theoretically, the values of ΔE_{int} calculated for the t14(H$_2$O)$_6$ and t12(H$_2$O)$_6$ complexes were found to be $-119,1$ kJ mol^{-1} and -94.2 kJ mol^{-1} respectively. Assuming that ΔH_{int} for *trans*-1,2-CHDA is similar to that of the *cis*-isomer, the comparison between the

calculated and experimental values lead to the conclusion that the $Am(H_2O)_x$ complexes are a good approximation to study the hydration of neutral amines in aqueous solution.

Due to the strength of the $N^+–H\cdots O_w$ charge-assisted H-bonds, ΔE_{int} is by far the dominant term of $\Delta E_{complex}$ in the $CHA^+(H_2O)_3$ complex. The small positive value of ΔE_{ass} in this complex shows that the water association step is energetically unfavorable to complexation. In this respect, the charged amino group acts as a water structure breaker, while the neutral one acts as a water structure maker.

In the diamine complexes, the increase of the charge makes ΔE_{int} to become more negative and ΔE_{ass} to become more positive. In relative terms, $|\Delta E_{int}| >> |\Delta E_{ass}|$. Focusing on ΔE_{int}, one can see that the values calculated for the $CHDA^+(H_2O)_6$ complexes are more negative than the sum of those found for neutral and protonated monoamines (dotted line in Figure 2), unless an internal H-bond is formed, as happens in $t12^+(H_2O)_6$. A similar trend is observed for the $CHDA^{2+}(H_2O)_6$ complexes, though here the differences relative to twice of the value of ΔE_{int} obtained for $CHA^+(H_2O)_3$ (dashed line in Figure 2) are more pronounced. These results lead us to conclude that the $NH_3^+–NH_2$ and $NH_3^+–NH_3^+$ proximity strengthens the Am-water interactions, in contrast to what occurs when both groups are neutral.

3.2. NEDA, NBO and AIM analysis

A better characterization of the Am-water interaction and of the mutual influence between the amino groups can be achieved by evaluating the interaction energy for each individual Am-water pair $[\Delta E(Am\text{-}w_i)$, with $i = 1$ to 3 or 6$)]$ and decomposing this energy into physical meaning terms using the NEDA approach.

The terms considered in this decomposition scheme are the electrical interaction (EL), charge transference (CT) and core repulsion (CORE). The first involves the classical electrostatic and polarization interactions, the second quantifies the

stabilization energy arising from donor-acceptor orbital interactions, and the third accounts for the repulsion energy between filled orbitals of the two units as well as for the electron exchange and correlation affects [17, 19]. The application of the NEDA analysis to the Am-water pairs of the different complexes is summarized in Table 4. This table also includes the results from the application of this approach to the interaction of the amines with the water envelope.

In $CHA(H_2O)_3$, the interaction energy between the NH_2 group and the water molecule in which the OH group acts as a proton donor (w_1) amounts to -27.7 kJ mol^{-1}. The CT component, mainly attributed to the LpN (nitrogen lone-pair) $\rightarrow\sigma^*$OH (OH unfilled sigma orbital) orbital interaction, prevails over the electrical energy. This means that this H-bond has an accentuated covalent character [56]. As expected, the weak H-donor capacity of NH_2 leads to a less energetic Am-w_3 H-bond being formed, ΔE = -5.8 kJ mol^{-1}, in which both CT (mainly due to the LpO$\rightarrow\sigma^*$NH orbital overlap) and EL components have identical weights. It is interesting to see that this value is only 0.5 kJ mol^{-1} more negative than ΔE(Am-w_2) in which the interaction is not of the H-bonding type. Thus, the N–H$\cdots$O$_w$ H-bond is just slightly stronger than the $NH_2\cdots w_2$ van der Walls interaction.

As mentioned above, hydrogen bond cooperativity plays a key role in the stabilization of the $CHA(H_2O)_3$ complex. An energetic quantification of this effect on the Am-water interactions (ΔE_{coop}) can be estimated through the following difference:

$$\Delta E_{coop} = \Delta E_{int} - \sum\Delta E(\text{Am-}w_i) \tag{5}$$

From Table 4 it can see that the value of ΔE_{coop} represents 33% of ΔE_{int} and that it comes mostly from the charge transference component. Applying equation (5) to the neutral diamine complexes, a value similar to $CHA(H_2O)_3$ is found for the relative contribution of cooperativity in $t14(H_2O)_6$. However, smaller values are calculated for

13

c13$(H_2O)_6$ (18%) and t12$(H_2O)_6$ (27%). This reduction of the relative weight of cooperativity can account for the weakening of the Am-water interactions as the NH_2 groups become closer together.

The values of ΔE(A-w_i) calculated for the $CHA^+(H_2O)_3$ complex indicate that the mean energy of an isolated N^+–H⋯O H-bond is *ca.* − 62 kJ mol^{-1}, a figure that is approximately 2.2 times more negative than that calculated for the OH⋯N H-bond in the CHA$(H_2O)_3$ complex. As expected, the presence of the charge makes the H-bond to be predominantly of electrical in nature. For the $CHA^+(H_2O)_3$ complex the energy difference given by equation (5) is positive (+14.6 kJ mol^{-1}), which means that there is an H-bonding anticooperative effect in the NH_3^+ hydration layer. As no water–water H-bonds exist in this layer, the anticooperativity comes from the charge dispersion over the complex as the water molecules are sequentially connected to the NH_3^+ group [57]. Indeed, the NBO analysis shows that while in the formation of a single H-bond the natural charge of the hydrogen atom is +0.486, in the trihydrate the charge of the hydrogen atoms ranges from +0.468 to +0.472.

From what has been said, to quantify the cooperative effect along the water bridges in the monoprotonated diamine complexes it is necessary to correct equation (5) to account for the anticooperative contribution (ΔE_{acoop}):

$$\Delta E_{coop} = \Delta E_{int} - \sum \Delta E(A\text{-}w_i) - \Delta E_{acoop} \qquad (6)$$

This anticooperativity term is given by the difference between the energy of a cluster comprising the amine and the water molecules H-bonded to NH_3^+ and the sum of the corresponding ΔE values of the individual Am-water pairs. The values of ΔE_{acoop} were calculated to be +14.6 kJ mol^{-1} for t14$^+(H_2O)_6$ and c13$^+(H_2O)_6$ and +6.7 kJ mol^{-1} for t12$^+(H_2O)_6$. ΔE_{coop} estimated for the CHDA$^+(H_2O)_6$ complexes are included in Table

14

4. The results show that for these complexes, 10 to 14% of ΔE_{int} is attributed to the stabilizing effect of the H-bonding cooperativity on the Am-water interactions.

The hydrogen bonding cooperativity is not the only factor accounting for the intensification of the Am-water interactions in the $CHDA^+(H_2O)_6$ complexes. In fact, as clearly evidenced in Table 4, for some weakly or non H-bonded Am-water pairs, the calculated interaction energies are unexpectedly strongly negative. This happens with $\Delta E(Am-w_4)$ and $\Delta E(Am-w_6)$ in $t14^+(H_2O)_6$ and $c13^+(H_2O)_6$ and with $\Delta E(Am-w_2)$, $\Delta E(Am-w_4)$ and $\Delta E(Am-w_6)$ in $t12^+(H_2O)_6$. It can be inferred from these results that the strengthening of the Am-water interactions in the complexes under analysis is also as a consequence of attractive charge-dipole interactions.

When both amino groups are charged, the absolute values of $\sum\Delta E(Am-w_i)$ increases abruptly relative to twice of the value calculated for $CHA^+(H_2O)_6$. On average, this increase amounts to 37% in $t14^{2+}(H_2O)_6$, 40% in $c13^{2+}(H_2O)_6$ and 50% in $t12^{2+}(H_2O)_6$. These results are consistent with the vibrational data and also explain the high negative values of ΔE_{int} calculated for these isomers. An interpretation of the N^+–H$\cdots O_w$ H-bonds' strengthening caused by the charges approximation can be given by comparing the ionic character of the N^+–H bonds in the protonated monoamine and diprotonated diamines. This comparison has been carried out both for the complexes and isolated amines.

In the framework of the NBO theory, the ionic character of the N^+–H bonds can be evaluated from the hybrid composition of the σ_{N^+H} orbital [20]:

$$\sigma_{N^+H} = a_N\,(sp^\lambda)_N + a_H\,(s)_H \tag{6}$$

where a_N and a_H are the polarization coefficients of the hybrids and λ the hybridization label. The ionicity parameter (i_{N^+H}) is given by $|a_N^2 - a_H^2|$, providing $a_N^2 + a_H^2 = 1$ [20]. The values of i_{N^+H} calculated for the isolated amines (values in parentheses) and for the

complexes are shown in Table 5. Other ionicity descriptors can be given by the AIM theory [58]. Two relevant ones are the electron density at the N^+–H bond critical point (ρ_{BCP}) and the ratio between the distance of the BCP to the hydrogen atom (d_{BCP}) and the interatomic distance (d_{N-H}). In fact, as the bond becomes more ionic the electron density at the BCP decreases and the critical point is pushed towards the positively charged hydrogen atom. Both parameters have been included in Table 5. As expected, the increase of i_{N^+H} is accompanied by a decrease of ρ_{BCP} and $d_{BCP\cdots H}/d_{N-H}$. A linear correlation was found between i_{N^+H} and the two topological parameters ($i_{N^+H} = -2.823$ $\rho_{BCP} + 1.407$, $R=0.979$; $i_{N^+H} = -0.167$ $d_{BCP}/d_{N-H} + 0.306$, $R=0.974$).

In the isolated molecules the ionic character of the N^+–H bonds increases from CHA^+ to $CHDA^{2+}$ and within the diamines it also increases as the NH_3^+ groups approximate each other. Thus, one can conclude that the repulsion between the charges makes the N^+–H bonds to become globally more ionic, thus favoring the formation of stronger Am-water H-bonds. Exceptions to this general trend are found for a few bonds in $t12^{2+}$ (N^+–H_{1b} and N^+–H_{2b}) due to the unfavorable orientation of the respective dipoles relative to the NH_3^+ group. However, as shown in Table 5, this is largely compensated by the strong increase of the ionic character of the other bonds, particularly the N^+–H_{1c} and N^+–H_{2c} ones.

The ionic character of the N^+–H bonds is also affected by the formation of intermolecular H-bonds with the water molecules. In NBO language, the N^+–H$\cdots$O H-bonds are characterized by LpO$\rightarrow\sigma^*N^+$H electron transference. The repolarization of the σN^+H orbital resulting from the electron donation increases a_N and decreases a_H, thus increasing the bond ionicity [20, 54]. As shown in Table 5, the values of i_{N^+H} increase substantially upon complexation with water. Regarding the topological parameters, they are also very sensitive to the H-bond formation. The values of ρ_{BCP} and

$d_{\text{BCP}\cdots\text{H}}/d_{\text{N-H}}$ decrease substantially upon hydration. However, it is important to note that that the variations of all iconicity descriptors are almost constant [$\Delta i_{\text{N}^+\text{H}} \approx 0.03$, $\Delta\rho_{\text{BCP}} \approx$ -0.011, $\Delta(d_{\text{BCP}\cdots\text{H}}/d_{\text{N-H}}) \approx$ -0.0047]. Therefore, it can be concluded that the differences of ionicity among the N^+–H bonds are not greatly affected by the presence of water. They are really determined by the electrostatic interaction between the charges.

3. Conclusions

This article focused on understanding the effect of the amino groups' positional isomery on the Am-water interaction. To achieve this goal we have investigated the vibrational and energetic properties of the cyclohexylamine and cyclohexyldiamine hydrates in the neutral and protonated forms.

An isolated NH_2 group tends to originate with the water molecules a strong O_w–H$\cdots$N H-bond and a much weaker N-H$\cdots\text{O}_w$ one. The presence of a third water molecule leads to the formation of a cyclic structure stabilized by H-bonding cooperativity. In contrast, the NH_3^+ group forms three strong and anticooperative N^+–H$\cdots\text{O}_w$ H-bonds with the water molecules. No water-water H-bonds are found to exist.

The mutual influence between two NH_2 groups in the neutral diamine complexes only occurs when they occupy the 1,3- or 1,2-positions. This interference is made *via* the common hydration shell that is formed between the groups. The hydrogen bonding cooperativity in this shell strengthens the water-water interactions and weakens the Am-water ones.

Interference between a NH_2 and a NH_3^+ group arises even when both occupy the most remote positions in the cyclohexyl ring. Unlike the neutral diamines, in the monoprotonated diamine complexes this interference results in the reinforcement of the Am-water interactions. Besides the contribution of the H-bonding cooperativity along

the water bridges, long-range charge-dipole attractive forces also contribute to this intensification.

When both groups are charged, the electrostatic repulsion between them causes the N^+–H bonds to be more ionic, leading to the stronger H-bonds with the water molecules. This effect becomes more pronounced as the charges approximate each other.

From the energy values calculated for the different Am-water pairs the following sequence of H-bonds' strengths could be established: N^+–H$\cdots O_w$ > O_w–H$\cdots$N >> N^+–H$\cdots O_w$. NEDA analysis revealed that in the first H-bond the electrical component prevails over the charge transference one whilst in the second the last component plays the major role. In the weakest H-bond the contribution of both components was found to be similar.

References

[1] A. Gugliucci, Polyamines as clinical laboratory tools, Clin. Chim. Acta, 344 (2004) 23-35.

[2] R.A. Casero, L.J. Marton, Targeting polyamine metabolism and function in cancer and other hyperproliferative diseases, Nat. Rev. Drug Discov., 6 (2007) 373-390.

[3] C. Moinard, L. Cynober, J.-P. de Bandt, Polyamines: metabolism and implications in human diseases, Clin. Nutr., 24 (2005) 184-197.

[4] D. Lucet, T. Le Gall, C. Mioskowski, The Chemistry of Vicinal Diamines, Angew. Chem.-Int. Edit., 37 (1998) 2580-2627.

[5] E. Jucker, E. Michalson, J. Szmuszkovicz, Medicinal agents incorporating the 1,2-diamine functionality, Progress in Drug Research, Springer Basel1989, pp. 135-149.

[6] F. Fache, E. Schulz, M.L. Tommasino, M. Lemaire, Nitrogen-Containing Ligands for Asymmetric Homogeneous and Heterogeneous Catalysis, Chem. Rev., 100 (2000) 2159-2232.

[7] C.C. Reviews, K. Wichmann, B. Antonioli, T. Söhnel, M. Wenzel, K. Gloe, K. Gloe, J.R. Price, L.F. Lindoy, A.J. Blake, M. Schröder, Polyamine-based anion receptors: Extraction and structural studies, Coord. Chem. Rev., 250 (2006) 2987-3003.

[8] Medina MA, Urdiales JL, Rodríguez-Caso C, Ramírez FJ, S.-J. F, Biogenic Amines and Polyamines: Similar Biochemistry for Different Physiological Missions and Biomedical Applications, Crit. Rev. Biochem. Mol. Biol., 38 (2003) 23-59.

[9] S.R.S. Saibabu Kotti, C. Timmons, G. Li, Vicinal Diamino Functionalities as Privileged Structural Elements in Biologically Active Compounds and Exploitation of their Synthetic Chemistry, Chem. Biol. Drug. Des., 67 (2006) 101-114.

[10] A.J. Lopes Jesus, L.I.N. Tomé, M.E.S. Eusébio, M.T.S. Rosado, J.S. Redinha, Hydration of Cyclohexylamines: CPCM Calculation of Hydration Gibbs Energy of the Conformers, J. Phys. Chem. A, 111 (2007) 3432-3437

[11] A.J. Lopes Jesus, M.H. S. F. Teixeira, J.S. Redinha, Structure of Charged Cyclohexyldiamines in Aqueous Solution: A Theoretical and Experimental Study, J. Phys. Chem. B, 116 (2012) 5019-5027.

[12] A.T. Blades, J.S. Klassen, P. Kebarle, Determination of Ion-Solvent Equilibria in the Gas Phase. Hydration of Diprotonated Diamines and Bis(trimethylammonium) Alkanes, J. Am. Chem. Soc., 118 (1996) 12437-12442.

[13] J.S. Klassen, A.T. Blades, P. Kebarle, Gas Phase Ion-Molecule Equilibria Involving Ions Produced by Electrospray. Hydration of Doubly Protonated Diamines, J. Am. Chem. Soc., 116 (1994) 12075-12076.

[14] J.S. Klassen, A.T. Blades, P. Kebarle, Determinations of Ion-Molecule Equilibria Involving Ions Produced by Electrospray. Hydration of Protonated Amines, Diamines, and Some Small Peptides, J. Phys. Chem., 99 (1995) 15509-15517.

[15] J.J. Dannenberg, L.K. Vinson, AM1 molecular orbital study of hydrogen bonding: gas-phase hydration of protonated diamines, J. Phys. Chem., 92 (1988) 5635-5639.

[16] A.J. Lopes Jesus, J.A.S. Almeida, A.A.C.C. Pais, J.S. Redinha, Molecular Dynamics and Quantum-Chemical Approaches in the Study of the Hydration of Protonated Cyclohexyldiamines Mol. Phys., (2013) DOI:10.1080/00268976.00262013.00805848.

[17] E.D. Glendening, Natural Energy Decomposition Analysis:An Extension to Density Functional Methods and Analysis of Cooperative Effects in Water Clusters, J. Phys. Chem. A, 109 (2005) 11936-11940.

[18] G.K. Schenter, E.D. Glendening, Natural Energy Decomposition Analysis: The Linear Response Electrical Self Energy, J. Phys. Chem., 100 (1996) 17152-17156.

[19] E.D. Glendening, Natural Energy Decomposition Analysis: Explicit Evaluation of Electrostatic and Polarization Effects with Application to Aqueous Clusters of Alkali Metal Cations and Neutrals, J. Am. Chem. Soc., 118 (1996) 2473-2482.

[20] F. Weinhold, C.R. Landis, Valency and bonding: A Natural Bond Orbital Donor–Acceptor Perspective, Cambridge University Press, New York, 2005.

[21] A.E. Reed, L.A. Curtiss, F. Weinhold, Intermolecular interactions from a natural bond orbital, donor-acceptor viewpoint, Chem. Rev., 88 (1988) 899-926.

[22] I.V. Alabugin, M. Manoharan, S. Peabody, F. Weinhold, Electronic Basis of Improper Hydrogen Bonding: A Subtle Balance of Hyperconjugation and Rehybridization, J. Am. Chem. Soc., 125 (2003) 5973-5987.

[23] A.D. Becke, Density-Functional Thermochemistry .3. The Role of Exact Exchange, J. Chem. Phys., 98 (1993) 5648-5652.

[24] C.T. Lee, W.T. Yang, R.G. Parr, Development of the Colle-Salvetti Correlation-Energy Formula into a Functional of the Electron-Density, Phys. Rev. B, 37 (1988) 785-789.

[25] A.D. Becke, Density-Functional Exchange-Energy Approximation with Correct Asymptotic-Behavior, Phys. Rev. A, 38 (1988) 3098-3100.

[26] D.E. Woon, J. Dunning, Thom H., Gaussian basis sets for use in correlated molecular calculations. III. The atoms aluminum through argon, J. Chem. Phys., 98 (1993) 1358-1371.

[27] J. Dunning, Thom H., Gaussian basis sets for use in correlated molecular calculations. I. The atoms boron through neon and hydrogen, J. Chem. Phys., 90 (1989) 1007-1023.

[28] S.F. Boys, F. Bernardi, The calculation of small molecular interactions by the differences of separate total energies. Some procedures with reduced errors, Mol. Phys., 19 (1970) 553-566.

[29] P. Sinha, S.E. Boesch, C. Gu, R.A. Wheeler, A.K. Wilson, Harmonic Vibrational Frequencies:Scaling Factors for HF, B3LYP, and MP2 Methods in Combination with Correlation Consistent Basis Sets, J. Phys. Chem. A, 108 (2004) 9213-9217.

[30] A.P. Scott, L. Radom, Harmonic Vibrational Frequencies: An Evaluation of Hartree−Fock, Møller−Plesset, Quadratic Configuration Interaction, Density Functional Theory, and Semiempirical Scale Factors, J. Phys. Chem., 100 (1996) 16502-16513.

[31] J.P. Merrick, D. Moran, L. Radom, An Evaluation of Harmonic Vibrational Frequency Scale Factors, J. Phys. Chem. A, 111 (2007) 11683-11700.

[32] M.J. Frisch, G.W. Trucks, H.B. Schlegel, G.E. Scuseria, M.A. Robb, J.R. Cheeseman, J.A. Montgomery Jr, T. Vreven, K.N. Kudin, J.C. Burant, J.M. Millam, S.S. Iyengar, J. Tomasi, V. Barone, B. Mennucci, M. Cossi, G. Scalmani, N. Rega, G.A. Petersson, H. Nakatsuji, M. Hada, M. Ehara, K. Toyota, R. Fukuda, J. Hasegawa, M. Ishida, T. Nakajima, Y. Honda, O. Kitao, H. Nakai, M. Klene, X. Li, J.E. Knox, H.P. Hratchian, J.B. Cross, V. Bakken, C. Adamo, J. Jaramillo, R. Gomperts, R.E. Stratmann, O. Yazyev, A.J. Austin, R. Cammi, C. Pomelli, J.W. Ochterski, P.Y. Ayala, K. Morokuma, G.A. Voth, P. Salvador, J.J. Dannenberg, V.G. Zakrzewski, S. Dapprich, A.D. Daniels, M.C. Strain, O. Farkas, D.K. Malick, A.D. Rabuck, K. Raghavachari, J.B. Foresman, J.V. Ortiz, Q. Cui, A.G. Baboul, S. Clifford, J. Cioslowski, B.B. Stefanov, G. Liu, A. Liashenko, P. Piskorz, I. Komaromi, R.L. Martin, D.J. Fox, T. Keith, M.A. Al-Laham, C.Y. Peng, A. Nanayakkara, M. Challacombe, P.M.W. Gill, B. Johnson, W. Chen, M.W. Wong, C. Gonzalez, J.A. Pople, *Gaussian 03*, revision D.01, Gaussian, Inc., Wallingford, CT, 2004.

[33] R. Dennington II, T. Keith, J. Millam, GaussView, Semichem, Inc, Shawnee Mission, KS, 2007.

[34] E.D. Glendening, J.K. Badenhoop, A.E. Reed, J.E. Carpenter, J.A. Bohmann, C.M. Morales, F. Weinhold, NBO 5.G, Theoretical Chemistry Institute, University of Wisconsin, Madison, WI, 2001.

[35] M.W. Schmidt, K.K. Baldridge, J.A. Boatz, S.T. Elbert, M.S. Gordon, J.H. Jensen, S. Koseki, N. Matsunaga, K.A. Nguyen, S. Su, T.L. Windus, M. Dupuis, J.A. Montgomery, General atomic and molecular electronic structure system, J. Comput. Chem., 14 (1993) 1347-1363.

[36] R.F.W. Bader, AIMPAC, Suite of programs for the Theory of Atoms in Molecules, McMaster University, Hamilton, Ontario, Canada, 1991.

[37] F.W. Biegler-König, R.F.W. Bader, W.-H. Tang, Calculation of the average properties of atoms in molecules. II, J. Comput. Chem., 3 (1982) 317-328.

[38] M. Mautner, The ionic hydrogen bond and ion solvation. 2. Solvation of onium ions by one to seven water molecules. Relations between monomolecular, specific, and bulk hydrogen, J. Am. Chem. Soc., 106 (1984) 1265-1272.

[39] M. Meot-Ner, P. Hamlet, E.P. Hunter, F.H. Field, Internal and external solvation of polyfunctional ions, J. Am. Chem. Soc., 102 (1980) 6393-6399.

[40] K.-Y. Kim, H.-C. Chang, Y.T. Lee, U.-I. Cho, D.W. Boo, Vibrational Predissociation Spectroscopic and Ab Initio Theoretical Studies on Protonated Ethylenediamine−(Water)$_3$ Complex, J. Phys. Chem. A, 107 (2003) 5007-5013.

[41] T. Steiner, The hydrogen bond in the solid state, Angew. Chem.-Int. Edit., 41 (2002) 48-76.

[42] M. Rozenberg, A. Loewenschuss, Y. Marcus, An empirical correlation between stretching vibration redshift and hydrogen bond length, Phys. Chem. Chem. Phys., 2 (2000) 2699-2702.

[43] A.V. Iogansen, Direct proportionality of the hydrogen bonding energy and the intensification of the stretching ν(XH) vibration in infrared spectra, Spectrochim. Acta A, 55 (1999) 1585-1612.

[44] P.L. Huyskens, Factors governing the influence of a first hydrogen bond on the formation of a second one by the same molecule or ion, J. Am. Chem. Soc., 99 (1977) 2578-2582.

[45] S.S. Xantheas, Cooperativity and hydrogen bonding network in water clusters, Chem. Phys., 258 (2000) 225-231.

[46] I. Alkorta, F. Blanco, P. Deyà, J. Elguero, C. Estarellas, A. Frontera, D. Quinonero, Cooperativity in multiple unusual weak bonds, Theoretical Chemistry Accounts, 126 (2010) 1-14.

[47] O. Mó, M. Yáñez, J. Elguero, Cooperative (nonpairwise) effects in water trimers: An ab initio molecular orbital study, J. Chem. Phys., 97 (1992) 6628-6638.

[48] L. González, O. Mó, M. Yáñez, J. Elguero, Cooperative effects in water trimers. The performance of density functional approaches, J. Mol. Struct. (Theochem), 371 (1996) 1-10.

[49] L. González, O. Mó, M. Yáñez, High level ab initio and density functional theory studies on methanol--water dimers and cyclic methanol(water)[sub 2] trimer, The Journal of Chemical Physics, 109 (1998) 139-150.

[50] L. González, O. Mó, M. Yáñez, Density functional theory study on ethanol dimers and cyclic ethanol trimers, J. Chem. Phys., 111 (1999) 3855-3861.

[51] G. Gilli, P. Gilli, The Nature of the Hydrogen Bond: Outline of a Comprehensive Hydrogen Bond Theory, Oxford University Press, New York, 2009.

[52] G. Gilli, P. Gilli, Towards an unified hydrogen-bond theory, J. Mol. Struct., 552 (2000) 1-15.

[53] P. Gilli, G. Gilli, Hydrogen bond models and theories: The dual hydrogen bond model and its consequences, J. Mol. Struct., 972 (2010) 2-10.

[54] A.J. Lopes Jesus, J.S. Redinha, Charge-Assisted Intramolecular Hydrogen Bonds in Disubstituted Cyclohexane Derivatives, J. Phys. Chem. A, 115 (2011) 14069-14077.

[55] L.I.N. Tomé, A.J. Lopes Jesus, R.A.E. de Castro, M.H.S.F. Teixeira, J. Canotilho, M.E.S. Eusébio, Solvation enthalpy and the thermodynamics of hydration of trans-cyclohexyl-1,4-diamine and cis-cyclohexyl-1,2-diamine, J. Chem. Thermodyn., 39 (2007) 1357-1362.

[56] S.a.J. Grabowski, What Is the Covalency of Hydrogen Bonding?, Chem. Rev., 111 (2011) 2597-2625.

[57] D. Liu, T. Wyttenbach, M.T. Bowers, Hydration of protonated primary amines: effects of intermolecular and intramolecular hydrogen bonds, Int. J. Mass spectrom., 236 (2004) 81-90.

[58] R.F.W. Bader, Atoms in Molecules - A Quantum Theory, University Press, Oxford, 1990.

Table 1. Wavenumbers (cm^{-1}), intensities (km mol^{-1}) and approximate description of the stretching vibration modes involving the hydroxyl and amino groups in the CHA(H$_2$O)$_3$ and CHDA(H$_2$O)$_6$ complexes.[a]

Complex	ν / cm^{-1}	Int. / (km mol^{-1})	Approximate description
CHA(H$_2$O)$_3$	3754.1−3743.4	64.9−50.1	ν(OH)$_{free}$
	3409.1	24.8	ν_{as}(NH$_2$)
	3382.7	633.6	ν(O$_3$H)
	3297.0	633.4	ν(O$_2$H) + ν_s(NH$_2$) op
	3282.7	354.3	ν(O$_2$H) + ν_s(NH$_2$) ip
	2996.9	1485.8	ν(O$_1$H)
t14(H$_2$O)$_6$	3755.1−3741.2	65.9−53.9	ν(OH)$_{free}$
	3411.5	27.1	ν_{as}(NH$_2$)$_1$
	3410.8	28.8	ν_{as}(NH$_2$)$_2$
	3382.5	511.5	ν(O$_3$H)
	3381.2	726.1	ν(O$_6$H)
	3302.0	863.3	ν(O$_5$H) + ν_s(NH$_2$)$_2$ op
	3298.7	640.5	ν(O$_2$H) + ν_s(NH$_2$)$_1$ op
	3285.8	294.5	ν(O$_5$H) + ν_s(NH$_2$)$_2$ ip
	3284.7	188.0	ν(O$_2$H) + ν_s(NH$_2$)$_1$ ip
	3002.9	742.4	ν(O$_1$H) + ν(O$_4$H) ip
	2996.6	2167.4	ν(O$_1$H) + ν(O$_4$H) op
c13(H$_2$O)$_6$	3756.2−3747.8	71.4−65.6	ν(OH)$_{free}$
	3499.0	190.1	ν(O$_5$H) + ν(O$_6$H) ip
	3496.8	518.4	ν(O$_5$H) + ν(O$_6$H) op
	3446.9	6.3	ν_{as}(NH$_2$)$_1$
	3442.2	5.2	ν_{as}(NH$_2$)$_2$
	3415.5	440.5	ν(O$_3$H′)
	3398.7	768.0	ν(O$_1$H′)
	3367.8	6.3	ν_s(NH$_2$)$_2$
	3362.8	3.9	ν_s(NH$_2$)$_1$
	3330.7	1133.4	ν(O$_2$H) + ν(O$_3$H′′) + ν(O$_4$H)
	3304.4	1040.6	ν(O$_1$H′′) + ν(O$_3$H′′) + ν(O$_4$H)
	3254.1	371.1	ν(O$_2$H) + ν(O$_3$H′′)
	3232.7	805.6	ν(O$_1$H′′) + ν(O$_4$H)
t12(H$_2$O)$_6$	3774.3	78.7	ν_{as}(H$_2$O)$_{free}$
	3753.8	53.4	ν(O$_5$H)$_{free}$
	3753.2	55.0	ν(O$_4$H)$_{free}$
	3672.5	7.0	ν_s(H$_2$O)$_{free}$
	3574.4	392.7	ν(O$_2$H′)
	3513.6	896.5	ν(O$_1$H′) + ν(O$_3$H′) ip
	3485.6	344.4	ν(O$_1$H′) + ν(O$_3$H′) op
	3436.4	274.2	ν(O$_3$H′′)
	3435.6	147.6	ν_{as}(NH$_2$)$_2$
	3424.6	23.2	ν_{as}(NH$_2$)$_1$
	3352.3	464.7	ν(O$_1$H′′)
	3337.3	272.6	ν_s(NH$_2$)$_1$ + ν_s(NH$_2$)$_2$ ip
	3318.4	42.5	ν_s(NH$_2$)$_1$ + ν_s(NH$_2$)$_2$ op
	3242.1	1186.0	ν(O$_4$H)
	3169.0	1345.6	ν(O$_2$H′′)
	3115.2	349.6	ν(O$_5$H)

[a] Calculated wavenumbers are scaled by a scaling factor of 0.9698. Abbreviations: s, symmetric; as: antisymmetric, ip, in-phase; op, out-of-phase.

Table 2. Wavenumbers (cm^{-1}), intensities (km mol^{-1}) and approximate description of the stretching vibration modes involving the hydroxyl and amino groups in the CHA$^+$(H$_2$O)$_3$ and CHDA$^+$(H$_2$O)$_6$ complexes.[a]

Complex	ν / cm^{-1}	Int. / (km mol^{-1})	Approximate description
CHA$^+$(H$_2$O)$_3$	3767.8–3767.1	217.9–93.7	ν_{as}(H$_2$O)$_{free}$
	3672.3–3671.2	39.4–32.1	ν_s(H$_2$O)$_{free}$
	3168.7	632.6	ν_{as}(NH$_3^+$)
	3164.6	629.5	ν_{as}(NH$_3^+$)
	3117.1	404.5	ν_s(NH$_3^+$)
t14$^+$(H$_2$O)$_6$	3773.8–3670.2	115.6–80.9	ν_{as}(H$_2$O)$_{free}$
	3746.9–3744.6	106.2–50.0	ν(OH)$_{free}$
	3673.8–3673.2	36.9–15.4	ν_s(H$_2$O)$_{free}$
	3430.0	39.2	ν_{as}(NH$_2$)
	3350.8	152.4	ν(O$_1$H) + ν(O$_4$H) op
	3337.5	97.3	ν_s(NH$_2$)
	3294.6	1142.6	ν(O$_1$H) + ν(O$_4$H) ip
	3194.3	588.9	ν_{as}(N$^+$H$_{1b}$; N$^+$H$_{1c}$)
	3165.8	1090.4	ν(O$_5$H)
	3160.2	688.8	ν_s(N$^+$H$_{1b}$; N$^+$H$_{1c}$)
	3008.0	357.8	ν(N$^+$H$_{1a}$)
c13$^+$(H$_2$O)$_6$	3775.7–3770.4	107.9–86.4	ν_{as}(H$_2$O)$_{free}$
	3748.5–3720.3	112.9–69.2	ν(OH)$_{free}$
	3676.2–3673.3	36.2–20.5	ν_s(H$_2$O)$_{free}$
	3488.7	313.0	ν(O$_1$H) + ν(O$_4$H) ip
	3443.1	419.8	ν(O$_1$H) + ν(O$_4$H) op
	3410.1	46.4	ν_{as}(NH$_2$)
	3348.6	694.7	ν(O$_2$H)
	3328.3	133.7	ν_s(NH$_2$)
	3192.7	777.7	ν_{as}(N$^+$H$_{1a}$; N$^+$H$_{1c}$)
	3132.8	241.7	ν_s(N$^+$H$_{1a}$; N$^+$H$_{1c}$)
	3001.6	611.4	ν(N$^+$H$_{1b}$)
	2909.6	836.7	ν(O$_5$H)
t12$^+$(H$_2$O)$_6$	3775.3	82.1	ν_{as}(H$_2$O)$_{free}$
	3753.1–3748.4	169.3–81.4	ν(OH)$_{free}$
	3746.9	113.6	ν_{as}(H$_2$O)$_{free}$
	3743.1	86.6	ν(OH)$_{free}$
	3675.6	17.6	ν_s(H$_2$O)$_{free}$
	3654.4	15.3	ν_s(H$_2$O)$_{free}$
	3569.9	306.8	ν(O$_2$H) + ν(O$_4$H) ip
	3550.7	349.8	ν(O$_2$H) + ν(O$_4$H) op
	3433.2	77.6	ν_{as}(NH$_2$)
	3393.1	1628.5	ν(O$_1$H) + ν(O$_5$H) ip
	3384.2	43.6	ν(O$_1$H) + ν(O$_5$H) op
	3350.6	140.9	ν_s(NH$_2$)
	3177.4	374.9	ν(N$^+$H$_{1b}$)
	3040.0	904.8	ν_{as}(N$^+$H$_{1a}$; N$^+$H$_{1c}$)
	3017.8	832.3	ν_s(N$^+$H$_{1a}$; N$^+$H$_{1c}$)

[a] Calculated wavenumbers are scaled by a scaling factor of 0.9698. Abbreviations: s, symmetric; as: antisymmetric, ip, in-phase; op, out-of-phase.

24

Table 3. Wavenumbers (cm^{-1}), intensities (km mol^{-1}) and approximate description of the stretching vibration modes involving the hydroxyl and amino groups in the CHDA^{2+}(H$_2$O)$_6$ complexes.^{a}

	ν / cm^{-1}	Int. / (km mol^{-1})	Approximate description
t14^{2+}(H$_2$O)$_6$	3753.5–3751.7	410.8–147.2	ν_{as}(H$_2$O)$_{free}$
	3663.4–3661.5	118.1–82.7	ν_{s}(H$_2$O)$_{free}$
	3103.3	1423.6	ν_{as}(NH$_3^+$)$_1$ + ν_{as}(NH$_3^+$)$_2$ op
	3086.8	1588.6	ν_{as}(NH$_3^+$)$_1$ + ν_{as}(NH$_3^+$)$_2$ op
	3054.0	1140.6	ν_{s}(NH$_3^+$)$_1$ + ν_{s}(NH$_3^+$)$_2$ op
c13^{2+}(H$_2$O)$_6$	3753.7–3750.3	293.3–128.4	ν_{as}(H$_2$O)$_{free}$
	3663.3–3660.3	101.0–4.4	ν_{s}(H$_2$O)$_{free}$
	3104.6	1477.6	ν_{as}(NH$_3^+$)$_1$ + ν_{as}(NH$_3^+$)$_2$ ip
	3083.0	1263.3	ν_{as}(NH$_3^+$)$_1$ + ν_{as}(NH$_3^+$)$_2$ ip
	3079.7	99.4	ν_{as}(NH$_3^+$)$_1$ + ν_{as}(NH$_3^+$)$_2$ op
	3054.2	24.7	ν_{s}(NH$_3^+$)$_1$ + ν_{s}(NH$_3^+$)$_2$ ip
	3045.3	1293.7	ν_{s}(NH$_3^+$)$_1$ + ν_{s}(NH$_3^+$)$_2$ op
t12^{2+}(H$_2$O)$_6$	3752.1–3722.2	154.9–128.4	ν_{as}(H$_2$O)$_{free}$
	3662.4–3503.1	372.8–43.4	ν_{s}(H$_2$O)$_{free}$
	3285.2	239.1	ν(NH$_{2b}$)
	3082.6	675.7	ν(NH$_{1a}$)
	3036.1	848.3	ν_{as}(N$^+$H$_{1b}$; N$^+$H$_{1c}$)
	3025.0	593.6	ν_{s}(N$^+$H$_{1b}$; N$^+$H$_{1c}$)
	3019.4	801.8	ν_{as}(N$^+$H$_{2a}$; N$^+$H$_{2c}$)
	3005.7	180.9	ν_{s}(N$^+$H$_{2a}$; N$^+$H$_{2c}$)

^{a} Calculated wavenumbers are scaled by a scaling factor of 0.9698. Abbreviations: s, symmetric; as: antisymmetric, ip, in-phase; op, out-of-phase.

Table 4. Summary of the application of the NEDA approach to the complexes and to the different isolated Am-water pairs and quantification of the effect of cooperativity (ΔE_{coop}) on the Am-water interaction.[a]

	$\Delta E(A-w_i)$						$\sum \Delta E(Am-w_i)$	ΔE_{int}	ΔE_{coop}
	Am-w$_1$	Am-w$_2$	Am-w$_3$	Am-w$_4$	Am-w$_5$	Am-w$_6$			
CHA(H$_2$O)$_3$	-27.66	-5.27	-5.82				-38.74	-58.07	-19.33 (33%)
EL	-84.77	-6.61	-33.72				-125.10	-130.50	-5.40
CT	-123.39	-3.10	-36.90				-163.39	-181.21	-17.82
CORE	180.50	4.44	64.85				249.78	253.63	3.85
t14(H$_2$O)$_6$	-27.36	-5.36	-5.94	-28.03	-5.02	-6.57	-78.28	-117.70	-39.42 (33%)
EL	-84.31	-6.65	-34.35	-86.15	-6.69	-37.20	-255.35	-265.56	-10.21
CT	-123.01	-3.10	-37.57	-126.15	-3.22	-39.96	-333.00	-369.66	-36.66
CORE	179.95	4.39	65.98	184.31	4.85	70.54	510.03	517.52	7.49
c13(H$_2$O)$_6$	-21.51	-1.34	-21.00	-1.63	-3.85	-3.60	-52.93	-64.56	-11.63 (18%)
EL	-67.70	-7.53	-64.81	-8.16	-4.52	-4.14	-156.86	-154.77	2.09
CT	-86.36	-11.88	-81.67	-11.51	-1.88	-1.51	-194.81	-202.71	-7.90
CORE	132.55	18.12	125.48	17.99	2.59	2.01	298.74	292.92	-5.82
t12(H$_2$O)$_6$	-25.65	-24.27	-6.78	-3.01	-10.79	3.01	-67.49	-92.97	-25.48 (27%)
EL	-63.35	-73.35	-8.45	-3.51	-64.85	2.80	-210.71	-219.28	-8.57
CT	-75.81	-97.82	-2.80	-1.55	-69.37	-0.71	-248.07	-270.91	-22.84
CORE	113.55	146.90	4.48	2.09	123.43	0.96	391.41	397.23	5.82
CHA$^+$(H$_2$O)$_3$	-60.88	-62.05	-62.05				-184.97	-170.33	
EL	-95.94	-95.69	-95.69				-287.32	-283.97	
CT	-85.31	-85.56	-85.56				-256.44	-254.85	
CORE	120.37	119.24	119.24				358.86	368.48	
t14$^+$(H$_2$O)$_6$	-57.61	-61.92	-62.13	-21.21	-27.78	-21.84	-252.50	-265.10	-27.23 (10%)
EL	-112.42	-93.72	-93.89	-32.22	-80.79	-45.86	-458.90	-469.74	-13.18
CT	-114.73	-82.59	-81.96	-17.99	-95.69	-35.94	-428.90	-445.39	-18.20
CORE	169.54	114.39	113.72	29.00	148.74	59.96	635.34	650.03	14.69
c13$^+$(H$_2$O)$_6$	-55.81	-59.50	-62.13	-18.79	-35.94	-22.34	-254.51	-273.13	-33.31 (12%)
EL	-100.25	-112.26	-93.43	-24.02	-103.14	-46.61	-479.70	-489.86	-13.14
CT	-86.78	-115.56	-82.30	-7.03	-139.16	-37.32	-468.15	-503.71	-37.53
CORE	131.17	168.32	113.64	12.26	206.35	61.59	693.33	720.44	17.41
t12$^+$(H$_2$O)$_6$	-57.11	-15.56	-10.75	-18.87	-59.50	-30.92	-192.72	-211.25	-25.27 (14%)
EL	-106.65	-15.82	-10.88	-19.33	-106.06	-51.46	-310.20	-333.67	-24.27
CT	-114.10	-1.00	-0.29	-1.13	-115.23	-37.28	-269.03	-276.14	-8.24
CORE	163.64	1.30	0.42	1.59	161.80	57.82	386.56	398.57	7.16
t14^{2+}(H$_2$O)$_6$	-82.80	-85.19	-85.19	-82.80	-85.19	-85.19	-506.35	-449.95	
EL	-116.19	-117.53	-117.53	-116.19	-117.53	-117.53	-702.49	-682.12	
CT	-97.45	-102.17	-102.17	-97.45	-102.17	-102.17	-603.58	-585.22	
CORE	130.83	134.52	134.52	130.83	134.52	134.52	799.73	817.39	
c13^{2+}(H$_2$O)$_6$	-84.98	-86.53	-86.53	-84.98	-86.53	-86.53	-516.05	-460.20	
EL	-118.16	-117.91	-117.91	-118.16	-117.91	-117.91	-707.93	-692.20	
CT	-99.16	-98.49	-98.49	-99.16	-98.49	-98.49	-592.29	-591.24	
CORE	132.34	129.91	129.91	132.34	129.91	129.91	784.33	823.24	
t12^{2+}(H$_2$O)$_6$	-94.10	-92.30	-95.27	-95.52	-83.09	-94.81	-555.09	-491.62	
EL	-125.27	-133.47	-127.82	-135.90	-92.93	-128.32	-743.71	-718.89	
CT	-102.80	-115.98	-114.68	-120.29	-40.67	-117.07	-611.49	-589.99	
CORE	134.01	157.15	147.28	160.71	50.46	150.58	800.19	817.26	

[a] All energy values are in kJ mol^{-1}. ΔE_{coop} was estimated from equations (5) and (6) for the neutral and protonated complexes, respectively. Values within parentheses represent the ratio between ΔE_{coop} and ΔE_{int} expressed as percentage.

Table 5. NBO and AIM Ionicity descriptors of the N^+–H bonds calculated for the hydrated and isolated CHA^+ and $CHDA^{2+}$ molecules.

Molecule	Bond	$\|i_{N^+H}\|^b$	$\rho_{BCP}{}^b$	$d_{BCP}/d_{N-H}{}^b$
CHA^+	N^+–H_{1a}	0.5024 (0.4698)	0.3208 (0.3303)	0.2260 (0.2310)
	N^+–H_{1b}	0.5046 (0.4706)	0.3209 (0.3310)	0.2257 (0.2314)
	N^+–H_{1c}	0.5046 (0.4706)	0.3209 (0.3310)	0.2257 (0.2314)
$t14^{2+}$	N^+–$H_{1a}{}^a$	0.5092 (0.4782)	0.3172 (0.3283)	0.2247 (0.2289)
	N^+–$H_{1b}{}^a$	0.5147 (0.4834)	0.3163 (0.3284)	0.2235 (0.2284)
	N^+–$H_{1c}{}^a$	0.5147 (0.4834)	0.3163 (0.3284)	0.2235 (0.2284)
$c13^{2+}$	N^+–$H_{1a}{}^a$	0.5097 (0.4788)	0.3167 (0.3282)	0.2245 (0.2288)
	N^+–$H_{1b}{}^a$	0.5192 (0.4806)	0.3148 (0.3277)	0.2227 (0.2276)
	N^+–$H_{1c}{}^a$	0.5117 (0.4879)	0.3173 (0.3286)	0.2243 (0.2290)
$t12^{2+}$	N^+–H_{1a}	0.5103 (0.4833)	0.3163 (0.3270)	0.2245 (0.2279)
	N^+–H_{1b}	0.5126 (0.4706)	0.3148 (0.3301)	0.2242 (0.2318)
	N^+–H_{1c}	0.5257 (0.4964)	0.3129 (0.3256)	0.2221 (0.2260)
	N^+–H_{2a}	0.5239 (0.4833)	0.3124 (0.3270)	0.2217 (0.2279)
	N^+–H_{2b}	0.4788 (0.4706)	0.3281 (0.3301)	0.2319 (0.2318)
	N^+–H_{2c}	0.5290 (0.4964)	0.3119 (0.3256)	0.2212 (0.2260)

[a] Because of symmetry similar values of the ionicity descriptors have been calculated for the NH_{2a}, NH_{2b} and NH_{2c} bonds. [b] Values in parentheses were calculated for the isolated molecules.

Captions of Figures

Figure 1. Structures of the $CHA(H_2O)_3$, $CHA^+(H_2O)_3$, $CHDA(H_2O)_6$, $CHDA^+(H_2O)_6$ and $CHDA^{2+}(H_2O)_6$ complexes optimized at the B3LYP/aug-cc-pVDZ level of theory including the atom numbering scheme. Prime and double prime symbols are used to distinguish hydrogen atoms of water molecules that are involved in different H-bonds. The optimized geometries of $CHA(H_2O)_3$, $CHA^+(H_2O)_3$, $CHDA^+(H_2O)_6$, and $CHDA^{2+}(H_2O)_6$ were taken from a previous authors' work [16].

Figure 2. Plot of the energies of complex formation and respective components given by equation (4) for the different complexes. The sequence of the diamine-water complexes from left to right is: t14, c13 and t12. For better visualization the negative energies are represented upwards and the positive ones downwards. The dot line represents the sum of the values of ΔE_{int} calculated for the $CHA(H_2O)_3$ and $CHA^+(H_2O)_3$ complexes and the dash line corresponds to twice of the value of ΔE_{int} calculated for the $CHA^+(H_2O)_3$ complex. The values of $\Delta E_{complex}$ for the $CHA(H_2O)_3$, $CHA^+(H_2O)_3$, $CHDA^+(H_2O)_6$, and $CHDA^{2+}(H_2O)_6$ were taken from a previous authors' work [16].
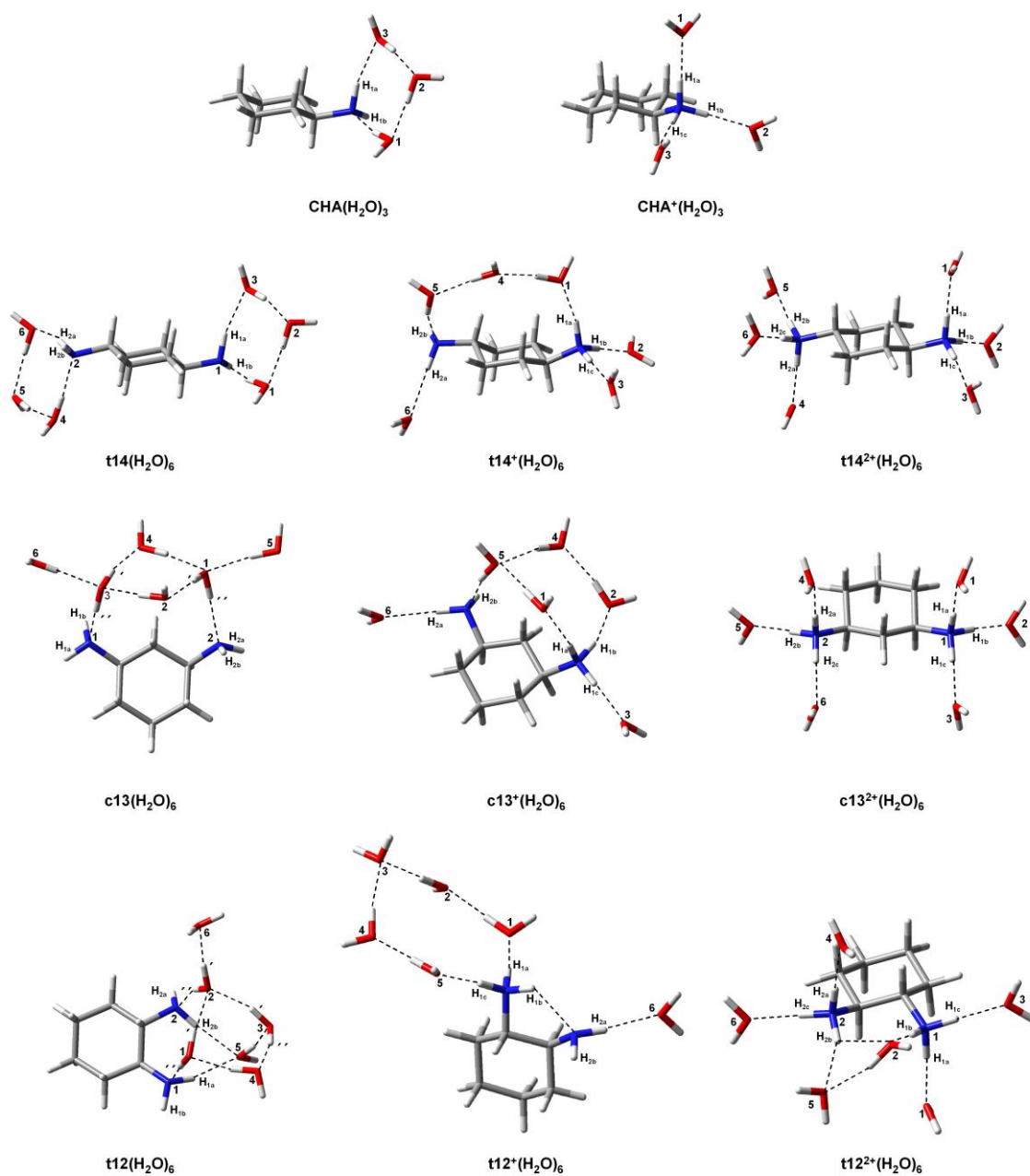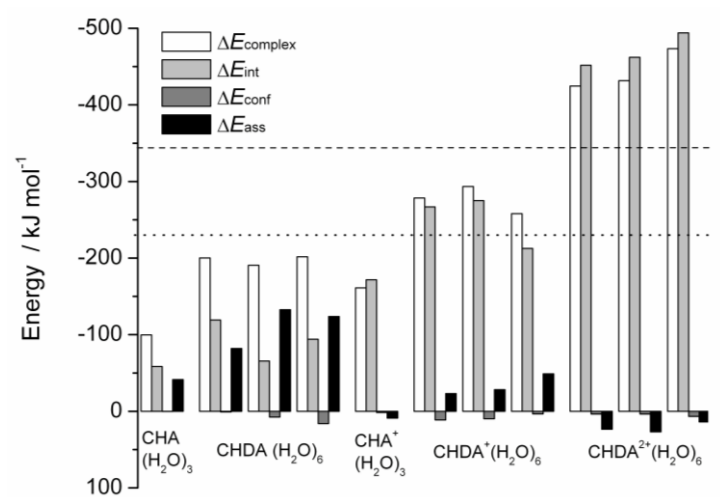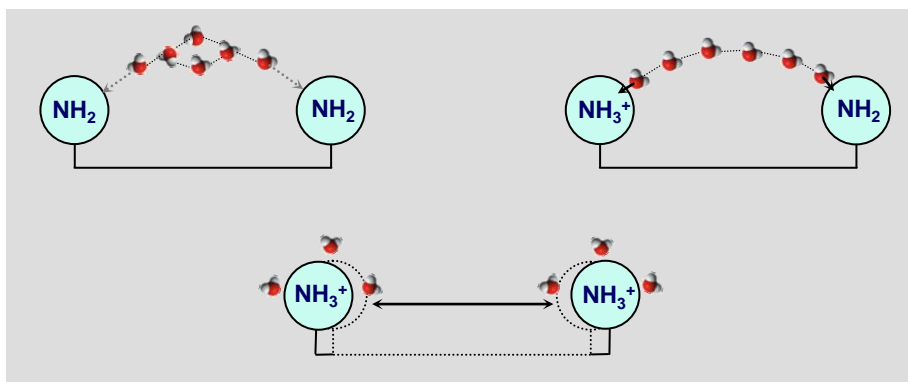
Figure 1

Figure 2

Graphical Abstract

Highlights

- The effect of the amino groups proximity on the amine-water interaction is studied
- Amine-water hydrogen bonds are characterized
- The contribution of water association and amine-water interaction is quantified
- Hydrogen bonding cooperativity plays an important role in the groups interference